A Group-Based Approach to Measuring Polarization

Supplementary Information

Isaac D. Mehlhaff*

July 7, 2023

Contents

*The University of North Carolina at Chapel Hill; mehlhaff@live.unc.edu.

S1 Analysis of Existing Literature

This section details the procedures and results of a simple exercise to gauge the use of various polarization measures in the political science literature. Journal articles were selected for the analysis if they satisfied two criteria: 1) Their title or abstract included any word with the root "polar," and 2) they were published between 2000 and 2021.[1] Polarization is an important concept throughout the social sciences but, for brevity and consistency, I focus on eight high-impact journals in political science. Four of these are general interest journals: *American Political Science Review*, *American Journal of Political Science*, *The Journal of Politics*, and *British Journal of Political Science*. The other four are subfield journals, selected to cover a wide range of subfields in which polarization is a prominent focus: *Public Opinion Quarterly*, *Legislative Studies Quarterly*, *Comparative Political Studies*, and *Political Analysis*. Table S1 describes the procedures used to obtain articles from each journal, including the database and search query used as well as any additional filters that needed to be applied to the results. These searches yielded a total of 322 articles.

Journal	Database	Search Query	Additional Filters	N
APSR	ProQuest	(ab(polariz*) AND PUBID(41041)) OR (ti(polariz*) AND PUBID(41041))	Date from 2000-01-01 to 2021-12-31	42
AJPS	JSTOR	polar* in Item Title field OR polar* in Abstract field	Date from 2000 to 2021, Journal is *American Journal of Political Science*	54
JOP	EBSCOhost Academic Search Premier	(TI(polar*) AND SO("the journal of politics")) OR (AB(polar*) AND SO("the journal of politics"))	Date from 01-2000 to 12-2021, Journal is *Journal of Politics*	71
BJPS	ProQuest	(ab(polariz*) AND PUBID(48551)) OR (ti(polariz*) AND PUBID(48551))	Date from 2000-01-01 to 2021-12-31	41
POQ	EBSCOhost Academic Search Premier	(TI(polar*) AND SO("public opinion quarterly")) OR (AB(polar*) AND SO("public opinion quarterly"))	Date from 01-2000 to 12-2021	39
LSQ	Wiley Online Library	polar* in Abstract field	Date from 1-2000 to 12-2021	35
CPS	SAGE Premier	polar* in Abstract field	Date from 2000 to 2021	27
PA	ProQuest	(ab(polariz*) AND PUBID(51675)) OR (ti(polariz*) AND PUBID(51675))	Date from 2000-01-01 to 2021-12-31	13

Table S1: Bibliometric Search Procedures

All types of scholarship—empirical, theoretical, and formal theoretical—were included, but the vast majority included at least some quantitative empirical analysis. After obtaining these 322 articles, I read each of them to determine how the authors operationalized polarization.[2] In most cases, this information was contained in the "Data and Measures" section, or another section titled similarly.[3]

Before presenting the results, a few words are in order with regard to coding rules. When possible, I attempted to group similar operationalizations together. The "difference" category subsumed any operationalization measuring the distance between observations or group means, or extremity as distance from

1. This excludes articles published online in "First View" or other similar pre-publication releases. That is, articles needed to be assigned an issue number to be included.

2. All articles except for one specified this information in the main text. This article was coded as "unspecified."

3. Eighty-two articles engaged with polarization theoretically but did not include it in any empirical analysis. These articles were coded as such and excluded from the calculations in Table S2.

a scale midpoint. Any operationalization measuring the sum of distances from an overall or group mean or otherwise measuring the cohesion of a group was coded as "variance." Both of these measures are often adjusted, for example, with party vote shares. Many authors attempt to capture some sense of bimodality with their measurement, with kurtosis and the Reynal-Querol index being popular choices; these are included under "bimodality." The finally category garnering an appreciable number of articles is that of "overlap;" there are several measures purporting to measure the degree to which two distributions (generally displayed as kernel density plots) overlap, and these are all subsumed under this category. Other categories contain, at most, a few articles and are generally self-explanatory. As articles often employ multiple operationalizations, I allow articles to be coded with more than one measure when appropriate. Proportions therefore may not sum to 1.

	APSR	*AJPS*	*JOP*	*BJPS*	*POQ*	*LSQ*	*CPS*	*PA*	**Overall**
Difference	0.548	0.63	0.62	0.512	0.538	0.629	0.333	0.615	**0.565**
Variance	0.19	0.13	0.099	0.195	0.077	0.057	0.259	0.154	**0.137**
Bimodality	0.048	0.037	0.014	0.049	0.026	0	0.074	0	**0.031**
Overlap	0	0.056	0	0.049	0.051	0.029	0	0.154	**0.031**
Correlation	0	0.037	0.014	0.098	0.026	0	0.037	0	**0.028**
Social Distance	0.071	0.019	0	0.024	0.077	0	0	0	**0.025**
Regression Coefficient	0	0	0.014	0.024	0.051	0.029	0	0	**0.016**
Proportion Extreme	0.024	0	0	0.024	0	0	0.074	0.077	**0.016**
Time	0	0	0	0.024	0	0.057	0	0	**0.009**
Party Unity	0	0.019	0	0	0	0.029	0	0	**0.006**
Party Votes	0	0	0.014	0	0	0	0.037	0	**0.006**
Divided Government	0	0	0	0.024	0	0	0.037	0	**0.006**
Coalition Size	0	0	0	0.024	0	0	0.037	0	**0.006**
Importance	0	0.019	0	0	0	0	0	0	**0.003**
R-Squared	0	0.019	0	0	0	0	0	0	**0.003**
Seat Proportion	0	0	0.014	0	0	0	0	0	**0.003**
Same-Party Clerk	0	0	0.014	0	0	0	0	0	**0.003**
Network Separation	0	0	0	0.024	0	0	0	0	**0.003**
Outparty Opinion	0	0	0	0	0.026	0	0	0	**0.003**
Engagement	0	0	0	0	0	0	0	0.077	**0.003**
Unspecified	0	0	0	0	0	0.029	0	0	**0.003**

Table S2: Proportion of Articles Using Polarization Measures

Table S2 displays the proportion of articles in each journal and overall that use each measure of polarization. Three patterns in the results characterize the state of polarization measurement in the political science literature. First, there is wide variability in how scholars attempt to tap into polarization—this simple analysis reveals no less than twenty distinct measurement strategies. In one sense, then, there is little consistency in measurement. In contrast, two measures—difference and variance—are substantially more common than all others, appearing in 56.5% and 13.7% of all articles, respectively. In this sense, then, there is great consistency in measurement. However, the reliability of past findings may be called into question if these two measures do not adequately capture polarization. Finally, there is some variation among subfields. In contrast to work in American politics, comparative scholarship tends to rely less on measures of difference and more on measures of variance, likely because the former complicates measurement in multi-party systems—a benefit to using the CPC that I show in the main text.

S2 Properties of the Measure

S2.1 Derivation

To derive the CPC, I begin by decomposing the total variance of clustered data (TSS) in (S1) into components directly corresponding to the two features of polarization: the variance accounted for between the clusters (BSS, corresponding to intergroup heterogeneity) and the variance accounted for within all clusters (WSS, corresponding to intragroup homogeneity). Dividing by TSS and solving for the BSS term gives an expression for the proportion of the total variance accounted for by the between-cluster variance—what I call the cluster-polarization coefficient (CPC):

$$\begin{aligned} TSS &= BSS + WSS, \\ \rightarrow CPC &= 1 - \frac{WSS}{TSS} = \frac{BSS}{TSS}. \end{aligned} \tag{S1}$$

More formally, I compute three terms in (S2): the total sum of squares TSS, the between-cluster sum of squares BSS, and the total within-cluster sum of squares WSS, where each individual i in cluster k holds a position on dimension j:

$$\begin{aligned} TSS &= \sum_{i=1}^{n_i} \sum_{j=1}^{n_j} (x_{ij} - \mu_j)^2, \\ BSS &= \sum_{k=1}^{n_k} \sum_{j=1}^{n_j} (\mu_{kj} - \mu_j)^2, \\ WSS &= \sum_{k=1}^{n_k} \sum_{i=1}^{n_i} \sum_{j=1}^{n_j} (x_{ikj} - \mu_{kj})^2. \end{aligned} \tag{S2}$$

Mirroring (S1), I arrive at formal expressions of the variance of clustered data and of the CPC in (S3). Expressed in this way, the CPC appears related—though not identical—to a one-way ANOVA F-statistic and the coefficient of determination (R^2).

$$
\begin{aligned}
TSS &= BSS + WSS, \\
\rightarrow \sum_{i=1}^{n_i}\sum_{j=1}^{n_j}(x_{ij}-\mu_j)^2 &= \sum_{k=1}^{n_k}\sum_{j=1}^{n_j}(\mu_{kj}-\mu_j)^2 + \sum_{k=1}^{n_k}\sum_{i=1}^{n_i}\sum_{j=1}^{n_j}(x_{ikj}-\mu_{kj})^2, \\
\rightarrow CPC &= 1 - \frac{\sum_{k=1}^{n_k}\sum_{i=1}^{n_i}\sum_{j=1}^{n_j}(x_{ikj}-\mu_{kj})^2}{\sum_{i=1}^{n_i}\sum_{j=1}^{n_j}(x_{ij}-\mu_j)^2}, \\
&= \frac{\sum_{k=1}^{n_k}\sum_{j=1}^{n_j}(\mu_{kj}-\mu_j)^2}{\sum_{i=1}^{n_i}\sum_{j=1}^{n_j}(x_{ij}-\mu_j)^2}, \\
&\forall \quad i \in (1,...,n_i), \quad j \in (1,...,n_j), \quad k \in (1,...,n_k).
\end{aligned}
\tag{S3}
$$

The CPC thus possesses two desirable properties: It is naturally bounded on the interval $[0, 1]$ and it takes into account both features of polarization. The CPC increases when the distance between groups increases or when groups become more tightly concentrated around their collective ideal point, but the rate of those increases depends on the relative levels of BSS and WSS.

As I show in section S3.3, however, this measure will be biased upward in small samples. To make the CPC more generalizable to contexts with varying numbers of observations, variables, and clusters, I incorporate corrections for lost degrees of freedom into the key variance expressions in (S4) and derive the adjusted CPC in (S5):

$$
\begin{aligned}
TSS_{adj} &= \frac{\sum_{i=1}^{n_i}\sum_{j=1}^{n_j}(x_{ij}-\mu_j)^2}{n_i - n_j}, \\
WSS_{adj} &= \frac{\sum_{k=1}^{n_k}\sum_{i=1}^{n_i}\sum_{j=1}^{n_j}(x_{ikj}-\mu_{kj})^2}{n_i - n_j n_k}.
\end{aligned}
\tag{S4}
$$

$$
\begin{aligned}
CPC_{adj} &= 1 - \frac{WSS_{adj}}{TSS_{adj}}, \\
\rightarrow CPC_{adj} &= 1 - \frac{\frac{\sum_{k=1}^{n_k}\sum_{i=1}^{n_i}\sum_{j=1}^{n_j}(x_{ikj}-\mu_{kj})^2}{n_i - n_j n_k}}{\frac{\sum_{i=1}^{n_i}\sum_{j=1}^{n_j}(x_{ij}-\mu_j)^2}{n_i - n_j}}, \\
&= 1 - \frac{\sum_{k=1}^{n_k}\sum_{i=1}^{n_i}\sum_{j=1}^{n_j}(x_{ikj}-\mu_{kj})^2}{\sum_{i=1}^{n_i}\sum_{j=1}^{n_j}(x_{ij}-\mu_j)^2}\frac{n_i - n_j}{n_i - n_j n_k}, \\
&= 1 - (1 - CPC)\frac{n_i - n_j}{n_i - n_j n_k}, \\
&\forall \quad i \in (1,...,n_i), \quad j \in (1,...,n_j), \quad k \in (1,...,n_k).
\end{aligned}
\tag{S5}
$$

S2.2 Distribution

Properties of the CPC can be further explored by deriving a sampling distribution. Because the CPC is effectively a ratio of two variances, an F statistic can be calculated:[4]

$$\begin{aligned} F &= \frac{\frac{BSS}{n_j n_k - n_j}}{\frac{WSS}{n_i - n_j n_k}}, \\ &= \frac{n_i - n_j n_k}{n_j n_k - n_j} \frac{TSS - WSS}{WSS}, \\ &= \frac{n_i - n_j n_k}{n_j n_k - n_j} \frac{TSS}{TSS} \frac{TSS - WSS}{WSS}, \\ &= \frac{n_i - n_j n_k}{n_j n_k - n_j} \frac{1 - \frac{WSS}{TSS}}{\frac{WSS}{TSS}}, \\ &= \frac{n_i - n_j n_k}{n_j n_k - n_j} \frac{1 - \frac{WSS}{TSS}}{1 - (1 - \frac{WSS}{TSS})}, \\ &= \frac{n_i - n_j n_k}{n_j n_k - n_j} \frac{CPC}{1 - CPC}. \end{aligned} \tag{S6}$$

where n_i, n_j, and n_k denote the number of observations, dimensions, and clusters, respectively; and $BSS \sim \chi^2(n_j n_k - n_j)$ and $WSS \sim \chi^2(n_i - n_j n_k)$ under the null hypothesis that $BSS - WSS = 0$. F is therefore distributed as a central $F(n_j n_k - n_j, n_i - n_j n_k)$ random variable. Solving for the CPC term from (S6) produces:

$$\begin{aligned} F &= \frac{n_i - n_j n_k}{n_j n_k - n_j} \frac{CPC}{1 - CPC}, \\ \rightarrow (n_j n_k - n_j) F - (n_j n_k - n_j)(CPC) F &= (n_i - n_j n_k) CPC, \\ \rightarrow (n_j n_k - n_j) F &= [(n_i - n_j n_k) + (n_j n_k - n_j) F] CPC, \\ \rightarrow CPC &= \frac{(n_j n_k - n_j) F}{(n_i - n_j n_k) + (n_j n_k - n_j) F}, \end{aligned} \tag{S7}$$

implying that $CPC \sim \text{Beta}(\frac{n_j n_k - n_j}{2}, \frac{n_i - n_j n_k}{2})$ under the null—a sensible result given that the CPC and the Beta distribution both have continuous support on the [0, 1] interval.

S2.3 Unbiasedness

From this distribution, it is straightforward to recover the mean:

4. This set-up and the proofs which follow are similar to the derivation of a sampling distribution for R^2 (Magee 1990).

$$\begin{aligned}\mathrm{E}(CPC) &= \frac{\frac{n_j n_k - n_j}{2}}{\frac{n_j n_k - n_j}{2} + \frac{n_i - n_j n_k}{2}}, \\ &= \frac{n_j n_k - n_j}{n_i - n_j}.\end{aligned} \tag{S8}$$

The unadjusted CPC is therefore asymptotically unbiased, again under the null hypothesis that $BSS - WSS = 0$, as $\lim_{n_i \to \infty} \mathrm{E}(CPC) = 0$. However, it will be biased upward in finite samples, and the degree of that bias will depend on both the number of dimensions and number of clusters, underscoring the need for the degrees-of-freedom corrections shown in section S3.1. Taking advantage of the expression in (S8), we can show that the adjusted CPC is, in fact, an unbiased estimator under the null:

$$\begin{aligned}\mathrm{E}(CPC_{adj}) &= \mathrm{E}[1 - (1 - CPC)\frac{n_i - n_j}{n_i - n_j n_k}], \\ &= 1 - \mathrm{E}[(1 - CPC)\frac{n_i - n_j}{n_i - n_j n_k}], \\ &= 1 - [\mathrm{E}(1 - CPC)]\frac{n_i - n_j}{n_i - n_j n_k}, \\ &= 1 - [1 - \mathrm{E}(CPC)]\frac{n_i - n_j}{n_i - n_j n_k}, \\ &= 1 - (1 - \frac{n_j n_k - n_j}{n_i - n_j})\frac{n_i - n_j}{n_i - n_j n_k}, \\ &= 1 - (\frac{n_i - n_j}{n_i - n_j} - \frac{n_j n_k - n_j}{n_i - n_j})\frac{n_i - n_j}{n_i - n_j n_k}, \\ &= 1 - (\frac{n_i - n_j n_k}{n_i - n_j})\frac{n_i - n_j}{n_i - n_j n_k}, \\ &= 1 - 1, \\ &= 0.\end{aligned} \tag{S9}$$

S2.4 Consistency

The variance of the CPC can also be recovered from its sampling distribution:

$$\begin{aligned}\text{Var}(CPC) &= \frac{\frac{n_j n_k - n_j}{2}\frac{n_i - n_j n_k}{2}}{(\frac{n_j n_k - n_j}{2} + \frac{n_i - n_j n_k}{2})^2(\frac{n_j n_k - n_j}{2} + \frac{n_i - n_j n_k}{2} + 1)}, \\ &= \frac{2(n_j n_k - n_j)(n_i - n_j n_k)}{(n_i - n_j)^2(n_i - n_j + 1)},\end{aligned} \tag{S10}$$

Taking advantage of (S10), we can also derive the variance of the adjusted CPC:

$$\begin{aligned}\text{Var}(CPC_{adj}) &= \text{Var}[1 - (1 - CPC)\frac{n_i - n_j}{n_i - n_j n_k}], \\ &= \text{Var}[(1 - CPC)\frac{n_i - n_j}{n_i - n_j n_k}], \\ &= (\frac{n_i - n_j}{n_i - n_j n_k})^2 \text{Var}(1 - CPC), \\ &= (\frac{n_i - n_j}{n_i - n_j n_k})^2 \text{Var}(CPC), \\ &= (\frac{n_i - n_j}{n_i - n_j n_k})^2 \frac{2(n_j n_k - n_j)(n_i - n_j n_k)}{(n_i - n_j)^2(n_i - n_j + 1)}, \\ &= \frac{2(n_j n_k - n_j)}{(n_i - n_j n_k)(n_i - n_j + 1)}.\end{aligned} \tag{S11}$$

The adjusted CPC is therefore consistent, as $\lim_{n_i \to \infty} \text{Var}(CPC_{adj}) = 0$.

S2.5 Additional Properties

Finally, I derive expressions for the median and mode of the sampling distribution. The median is presented in (S12), where I_x gives the regularized incomplete Beta function:[5]

$$\begin{aligned}\text{median}(CPC) &= I^{-1}_{\frac{1}{2}}(\frac{n_j n_k - n_j}{2}, \frac{n_i - n_j n_k}{2}), \\ &\approx \frac{\frac{n_j n_k - n_j}{2} - \frac{1}{3}}{\frac{n_j n_k - n_j}{2} + \frac{n_i - n_j n_k}{2} - \frac{2}{3}}, \\ &\approx \frac{3(n_j n_k - n_j) - 2}{3(n_i - n_j) - 4}.\end{aligned} \tag{S12}$$

The mode of the sampling distribution can be expressed as:

5. The solution given in (S12) is approximate—the median of the Beta distribution has no closed-form expression for arbitrary parameters.

$$\begin{aligned}\text{mode}(CPC) &= \frac{\frac{n_j n_k - n_j}{2} - 1}{\frac{n_j n_k - n_j}{2} + \frac{n_i - n_j n_k}{2} - 2} \\ &= \frac{n_j n_k - n_j - 2}{n_i - n_j - 4},\end{aligned} \tag{S13}$$

implying that the distribution possesses a unique and finite mode when $n_i - n_j > 4$ and $n_j n_k - n_j \geq 2$.

S3 Simulation Evidence

S3.1 Set-Up

In this section, I present evidence for the efficacy of the CPC by simulating both univariate and bivariate data using Gaussian mixture distributions. The purpose of this simulation exercise is to evaluate—in a controlled environment—the extent to which the CPC captures the two features of polarization, and whether it does so better than existing measures. Gaussian mixtures are uniquely suited for this purpose because they provide a straightforward method for mimicking distributional polarization. Each component of a Gaussian mixture is parameterized by a location parameter μ and scale parameter σ, which neatly correspond to the two features of polarization: intergroup heterogeneity and intragroup homogeneity, respectively.

Figure S1 presents a visualization of this intuition. This figure displays kernel density plots for simulated univariate data with two components. The plots are arranged such that the least polarized distributions fall at the top left and the most polarized distributions fall at the bottom right, and component parameters are provided by the plot labels along the top and right axes. Consider what happens to these component parameters as we move from a less polarized to a more polarized distribution. Moving from left to right across the rows of the facet plot, for example, the distributions become more polarized as the difference between component means increases and the components grow farther apart. Likewise, moving from top to bottom along the columns of the facet plot, the distributions become more polarized as component standard deviations decrease and the components grow more compact.

By manipulating these component parameters, therefore, I can generate mixture distributions with varying levels of polarization and estimate those levels using the CPC and other existing measures. I focus here on comparing the CPC to the two most popular strategies for measuring polarization in the political science literature: difference-in-means and variance. To identify the accuracy of each polarization measure, I examine the intergroup heterogeneity and intragroup homogeneity features separately. To simulate polarization as a result of increasing intergroup heterogeneity, I execute a four-step simulation exercise, randomly varying μ:

1. Fix component standard deviations at a range of values $\sigma \in \{0.5, 1, 1.5, 2\}$.[6] For identification, I use the same σ for each component and maintain a global mean of zero.

2. For each component standard deviation σ, select 1,000 values of μ as independent draws from $\text{U}(2, 5)$.

3. Take 1,000 independent draws from a Gaussian mixture parameterized by $\text{N}(-\mu, \sigma; \mu, \sigma)$.

6. As seen in Figure S1, even this relatively short range of values is sufficient to generate distributions ranging from unimodal to distinctly bimodal.

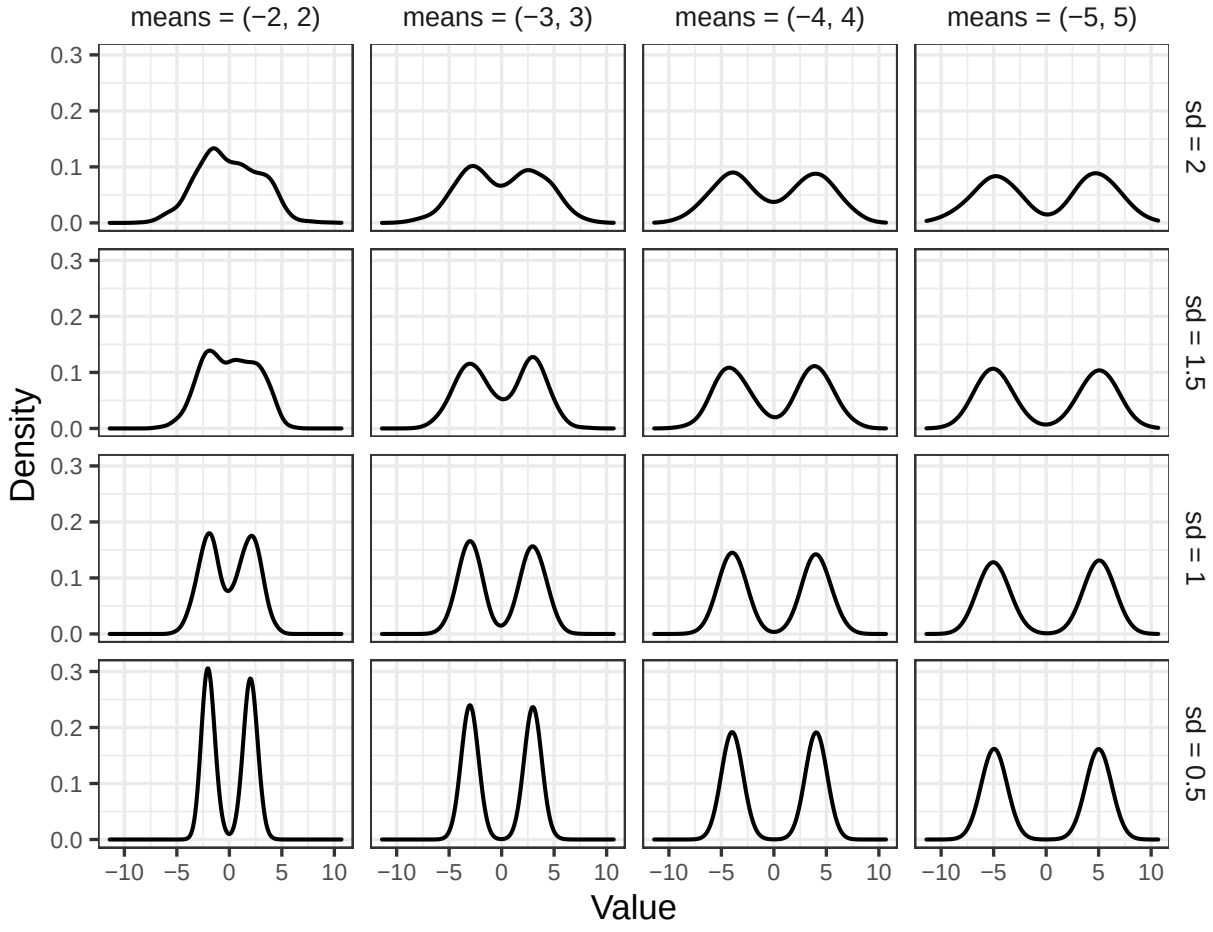

Figure S1: Visualization of Simulation Set-Up. Simulated Gaussian mixture distributions with $\mu_{global} = 0$; rows represent diverging means with standard deviations held constant and columns represent decreasing standard deviations with means held constant; thus, the least polarized distributions appear at top left and the most polarized distributions appear at bottom right.

4. Apply each polarization measure to the resulting distribution.

The result of this procedure is 1,000 distributions, each with $N = 1000$, with which to evaluate the performance of each polarization measure. To simulate polarization as a result of increasing intragroup homogeneity, I execute a similar four-step simulation exercise, randomly varying σ:

1. Fix component means at a range of values $\mu \in \{2, 3, 4, 5\}$.[7] For identification, I use the same absolute value of μ for each component and maintain a global mean of zero.

2. For each component mean μ, select 1,000 values of σ as independent draws from $\mathrm{U}(0.5, 2)$.

3. Take 1,000 independent draws from a Gaussian mixture parameterized by $\mathrm{N}(-\mu, \sigma; \mu, \sigma)$.

4. Apply each polarization measure to the resulting distribution.

7. Again, as seen in Figure S1, even this relatively short range of values is sufficient to generate distributions ranging from unimodal to distinctly bimodal.

The result of this procedure is 1,000 distributions, each with $N = 1000$, with which to evaluate the performance of each polarization measure. For identification, I use equal component weights across all simulated distributions.[8]

Using these simulation frameworks, I evaluate the performance of the adjusted CPC relative to difference and variance in both univariate and bivariate contexts.[9] Pursuant to the two definitional characteristics of polarization, an appropriate measure should indicate higher polarization when the distance between component means increases or when the standard deviation of each component decreases. Because polarization can occur around more than two poles, especially in multiparty systems, I conduct these procedures for distributions with two, three, and four components.[10] For all simulations, I calculate the adjusted CPC using true group memberships, which are known from the data randomization procedure. By using true group memberships instead of estimating them using a clustering algorithm, we can be sure that any advantages or disadvantages uncovered in the simulation results are attributable to the CPC itself and not to a clustering method being well- or ill-suited to this particular data structure.

S3.2 Results

I evaluate each simulated distribution using all three measures and present the results in two ways. First, Figures S2 and S3 present the raw polarization estimates as a function of the randomized parameters for two-component simulations with univariate and bivariate data, respectively.[11] All measures are scaled to $[0, 1]$ to enable comparison and plotted using locally estimated scatterplot smoothing (LOESS). A measure performing in line with theoretical expectations would register a positive slope in plot (a) and a negative slope in plot (b). However, the magnitude of those slopes and the absolute level of estimated polarization should differ depending on the fixed parameter. For example, the sets of distributions with fixed $\sigma = 0.5$ or fixed $\mu = (-5, 5)$ are more polarized on average than the distributions with a greater fixed σ or fixed μ parameters that are closer together. As a result, polarization estimates should generally be higher for those distributions and less sensitive to the value of the randomized parameter.

The results presented in Figures S2 and S3 generally align with expectations. Looking first at plot (a), slopes for difference, variance, and the adjusted CPC carry the expected sign. The magnitude of the difference and variance slopes, however, is relatively constant regardless of the fixed parameter, and the absolute level of estimated polarization appears similar. For example, with random component means of $(-5, 5)$ at the far right hand side of each facet, difference and variance output almost identical polarization estimates regardless of whether component standard deviations are 0.5, 2, or anywhere in between. The CPC, on the other hand, appears more sensitive to those fixed parameters and displays intercepts and slope magnitudes more in line with expectations.[12] The insensitivity of difference and variance to component standard deviations can be seen more clearly in plot (b). While the adjusted CPC again performs as expected, difference and variance

8. Additional simulations in Supplementary Information section S3.3 investigate how the CPC changes in response to varying component weights.

9. For bivariate data, I calculate difference by taking the average Euclidean distance between all component means, and I calculate variance as the trace of the covariance matrix.

10. For three and four components, I calculate the difference score by taking the average distance between all component means.

11. Supplementary Information section S3.1 contains results of three- and four-component simulations.

12. At extremely high levels of polarization (e.g. $\sigma = 0.5$), however, the CPC is likewise relatively insensitive to increasing the distance between component means. This may not be a desirable property if the intended use is to measure polarization when groups are extremely concentrated around their ideal point. However, Supplementary Information section S6.3 analyzes the relative weight each feature has on the CPC across a range of values plausible in real-world data, and results suggest this diminishing impact only occurs at very high levels of polarization.

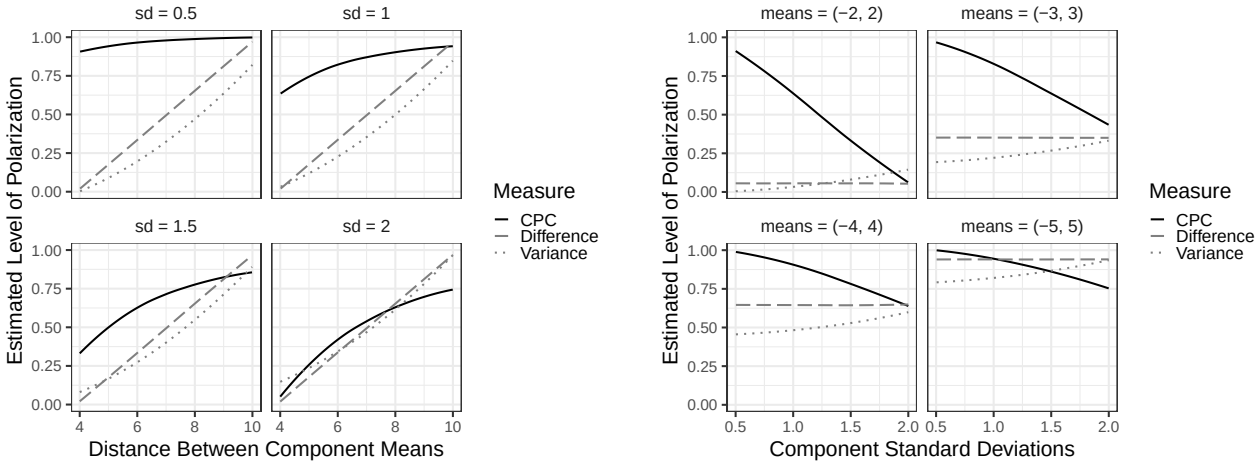

(a) Random μ (intergroup heterogeneity) (b) Random σ (intragroup homogeneity)

Figure S2: Univariate Polarization Estimates with Two Components. Results from univariate simulations of polarization measures with two components, showing estimated level of polarization for a randomly varying distribution parameter, holding the other parameter constant. All measures scaled to $[0, 1]$ to enable comparison and plotted using LOESS.

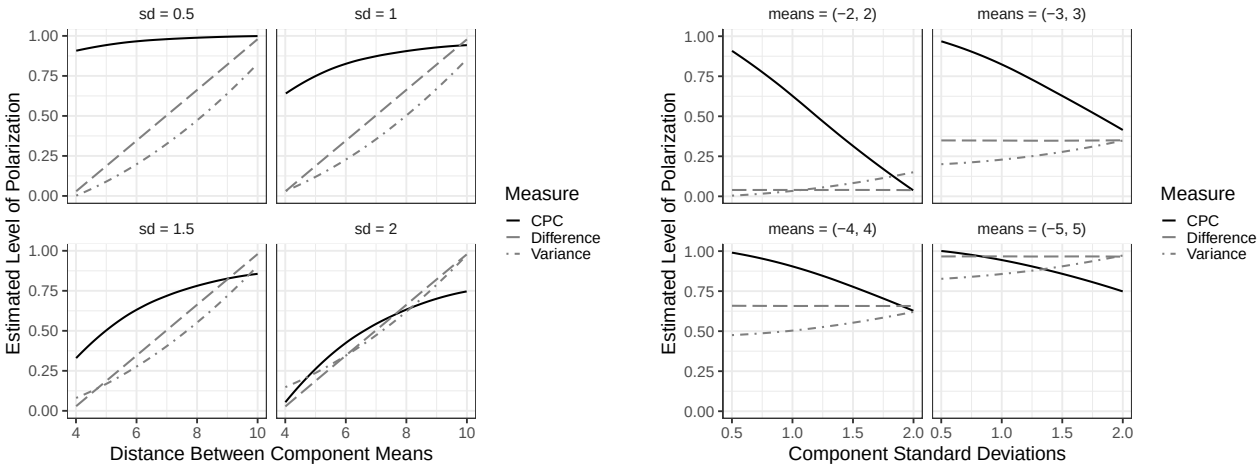

(a) Random μ (intergroup heterogeneity) (b) Random σ (intragroup homogeneity)

Figure S3: Bivariate Polarization Estimates with Two Components. Results from bivariate simulations of polarization measures with two components, showing estimated level of polarization for a randomly varying distribution parameter, holding the other parameter constant. All measures scaled to $[0, 1]$ to enable comparison and plotted using LOESS.

appear as nearly flat lines, although they do output higher polarization estimates when the difference between fixed component means grows larger.

Understanding how raw polarization estimates track with distributional characteristics is valuable, but it complicates a formal evaluation of a measure's effectiveness because the estimated level of polarization (the output of each measure) and the parameters controlling the simulated level of polarization (standard deviation or distance between means) are different quantities and are on different scales. Moreover, we do not have information about the "true" level of distributional polarization—estimating such quantities is the very goal of this measurement approach.[13]

By holding all other distributional characteristics constant and randomly varying only component means and standard deviations, however, we do have information about each distribution's level of polarization *relative* to every other distribution. For example, the simulation to assess the intergroup heterogeneity feature holds standard deviations constant and randomly varies component means. Randomly generated means that are further apart will generate a distribution that is, in theory, more polarized. The result of the simulation, then, is 1,000 distributions that randomly vary in their level of polarization, and those relative levels of polarization can be identified by the relative value of the random component means. I therefore follow the approach taken by Lupu, Selios, and Warner (2017) and use the estimated polarization from each measure to rank-order the distributions and compare those rankings to the true rank-order recovered from the randomized parameters, with a higher rank indicating a greater level of polarization.

Table S3 reports the root mean squared error (RMSE) and Spearman's rank correlation coefficient (rho) for all three measures across all simulations.[14] Bolded values represent the best-performing measure in each category. Examining these results, a clear pattern emerges. Difference and variance register the lowest error rates on the intergroup heterogeneity feature, regardless of the number of variables or components. This makes intuitive sense; holding the standard deviations of a mixture distribution constant and pulling the component means in opposite directions should, by definition, result in wider differences between means and higher variance for the distribution as a whole. The CPC performs as expected on both features and often improves slightly in higher dimensions and multimodal distributions, which enables comparison across a wider variety of contexts.

Finally, although it is necessary to examine each feature in isolation, real-world data rarely holds one feature constant while manipulating the other. When looking at each measure's respective overall performance, the CPC appears to perform best regardless of the number of variables or components, and often by a drastic margin.[15] As seen in Table S3, this performance gain appears to come from the CPC performing only slightly worse on the intergroup heterogeneity feature but dramatically better on the intragroup homogeneity feature.

13. Supplementary Information section S4 pursues another strategy for procuring "ground-truth" polarization estimates: using human coders to evaluate relative polarization levels.

14. This rank-order approach coerces all polarization measurements to an evenly spaced scale, thereby requiring an assumption of cardinality in the calculation of RMSE. This assumption can be relaxed in the case of Spearman's ρ, which is nonparametric.

15. Overall performance is calculated by simply combining results from the intergroup heterogeneity and intragroup homogeneity simulations and calculating error statistics over the entire body of evidence.

		Univariate			Bivariate		
		Difference	Variance	CPC	Difference	Variance	CPC
	$k = 2$						
RMSE	Intergroup Heterogeneity	**14.665**	15.384	30.731	**10.57**	11.2	21.999
	Intragroup Homogeneity	406.645	572.361	**24.009**	406.124	574.712	**16.786**
	Overall	287.729	404.866	**27.576**	287.271	406.46	**19.567**
Spearman's ρ	Intergroup Heterogeneity	**0.999**	0.999	0.994	**0.999**	0.999	0.997
	Intragroup Homogeneity	0.008	-0.966	**0.997**	0.01	-0.982	**0.998**
	Overall	0.503	0.016	**0.995**	0.505	0.009	**0.998**
	$k = 3$						
RMSE	Intergroup Heterogeneity	**17.704**	19.026	32.33	**12.148**	13.287	22.341
	Intragroup Homogeneity	400.398	573.837	**25.406**	405.765	575.339	**18.047**
	Overall	283.401	405.987	**29.075**	287.047	406.935	**20.307**
Spearman's ρ	Intergroup Heterogeneity	**0.998**	0.998	0.994	**0.999**	0.999	0.997
	Intragroup Homogeneity	0.038	-0.976	**0.996**	0.012	-0.986	**0.998**
	Overall	0.518	0.011	**0.995**	0.506	0.006	**0.998**
	$k = 4$						
RMSE	Intergroup Heterogeneity	**10.215**	10.392	28.948	**10.79**	11.571	21.808
	Intragroup Homogeneity	403.642	567.642	**21.499**	414.84	574.874	**17.35**
	Overall	285.51	401.451	**25.497**	293.436	406.58	**19.706**
Spearman's ρ	Intergroup Heterogeneity	**0.999**	0.999	0.995	**0.999**	0.999	0.997
	Intragroup Homogeneity	0.022	-0.933	**0.997**	-0.033	-0.983	**0.998**
	Overall	0.511	0.033	**0.996**	0.483	0.008	**0.998**

Table S3: Error of Distribution Rankings in Simulation. Root mean squared error and Spearman's ρ calculated for univariate and bivariate simulations with two, three, and four components; bolded values denote measure with lowest error in each category.

S3.3 Additional Plots

This section presents additional plots of simulation results, analogous to Figures S2 and S3 for the cases of three and four components.

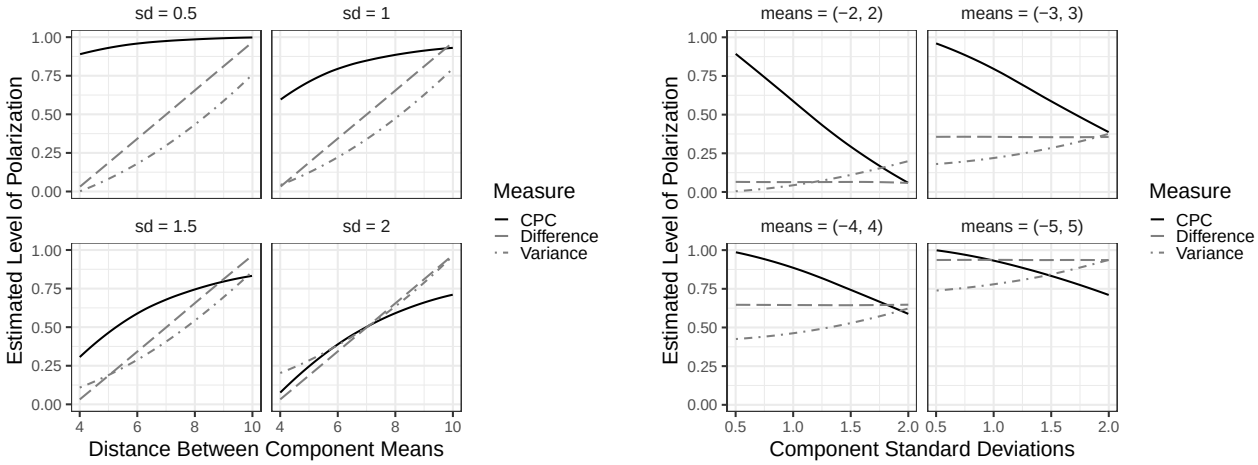

(a) Random μ (intergroup heterogeneity) (b) Random σ (intragroup homogeneity)

Figure S4: Univariate Polarization Estimates with Three Components Results from univariate simulations of polarization measures with three components, showing estimated level of polarization for a randomly varying distribution parameter, holding the other parameter constant. All measures scaled to $[0, 1]$ to enable comparison and plotted using LOESS.

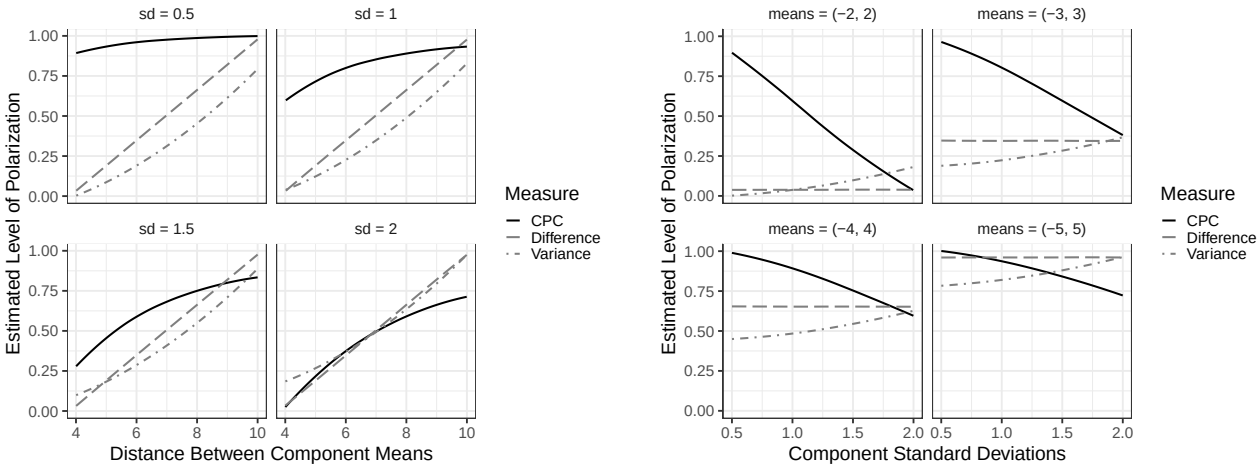

(a) Random μ (intergroup heterogeneity) (b) Random σ (intragroup homogeneity)

Figure S5: Bivariate Polarization Estimates with Three Components. Results from bivariate simulations of polarization measures with three components, showing estimated level of polarization for a randomly varying distribution parameter, holding the other parameter constant. All measures scaled to $[0, 1]$ to enable comparison and plotted using LOESS.

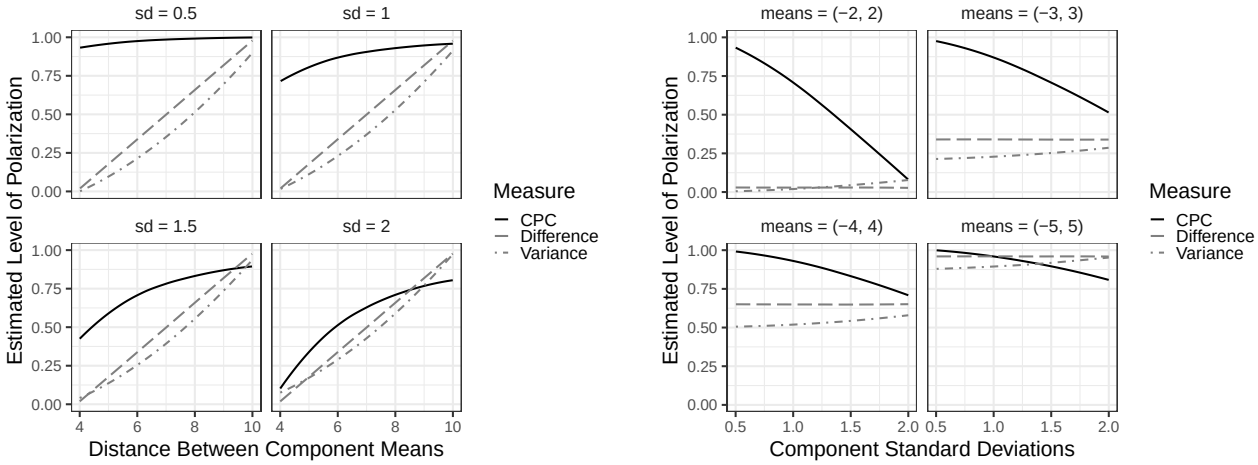

(a) Random μ (intergroup heterogeneity) (b) Random σ (intragroup homogeneity)

Figure S6: Univariate Polarization Estimates with Four Components. Results from univariate simulations of polarization measures with four components, showing estimated level of polarization for a randomly varying distribution parameter, holding the other parameter constant. All measures scaled to $[0, 1]$ to enable comparison and plotted using LOESS.

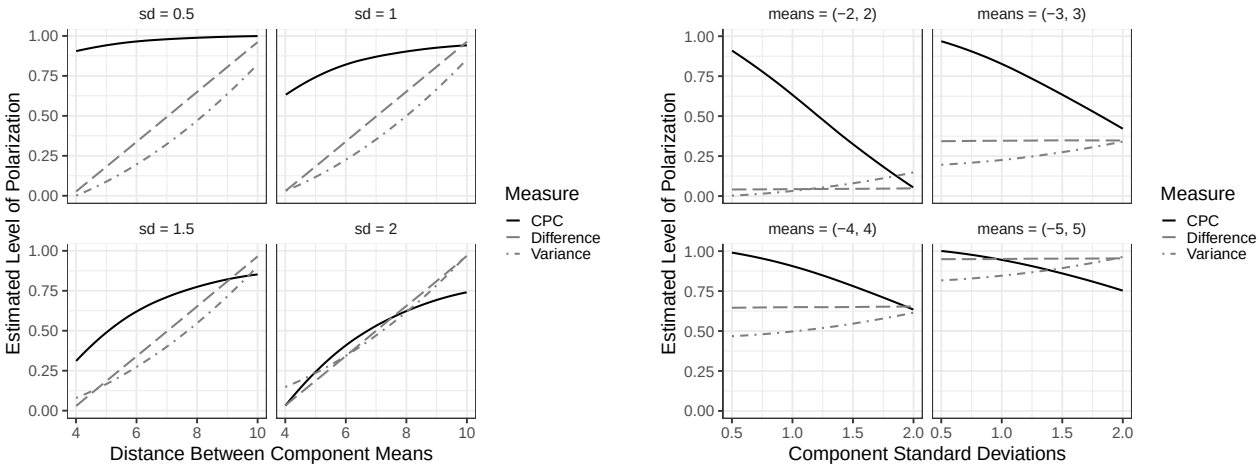

(a) Random μ (intergroup heterogeneity) (b) Random σ (intragroup homogeneity)

Figure S7: Bivariate Polarization Estimates with Four Components. Results from univariate simulations of polarization measures with four components, showing estimated level of polarization for a randomly varying distribution parameter, holding the other parameter constant. All measures scaled to $[0, 1]$ to enable comparison and plotted using LOESS.

S3.4 Results with Log-Normal Data

Constructing the CPC using sums of squares imposes an important limitation: It is sensitive to extreme outliers. Consider how this measure would respond to adding observations far out in the tails of a distribution. Such observations would lead to rapid increases in $TWSS$, likely overwhelming any increase in BSS that would result from small changes to the group's centroid. As a consequence, the CPC will rapidly decrease and remain relatively insensitive to any further changes in either variable, for the same reasons previously discussed. To demonstrate this limitation, I followed a simulation procedure similar to the one in section S4.1. Simulations to evaluate polarization measures on the intergroup heterogeneity feature follow the procedure below:

1. Fix component standard deviations at a range of values $\sigma \in \{e^{0.25}, e^{0.5}, e^{0.75}\}$. For identification, I use the same σ for each component.
2. For each component standard deviation σ, select 500 values of μ as independent draws from $\text{U}(e, e^3)$.
3. Take 500 independent draws from $\text{logN}(\mu, \sigma)$.
4. Reflect each data point over the y-axis to obtain a bimodal distribution with heavy tails on left and right.
5. Apply each polarization measure to the resulting distribution.

The result of this procedure is 1,000 heavy-tailed distributions, each with $N = 1000$. Simulations to evaluate polarization measures on the intragroup homogeneity feature follow the procedure below:

1. Fix component means at a range of values $\mu \in \{e, e^2, e^3\}$. For identification, I use the same absolute value of μ for each component.
2. For each component mean μ, select 500 values of σ as independent draws from $\text{U}(e^{0.25}, e^{0.75})$.
3. Take 500 independent draws from $\text{logN}(\mu, \sigma)$.
4. Reflect each data point over the y-axis to obtain a bimodal distribution with heavy tails on left and right.
5. Apply each polarization measure to the resulting distribution.

The result of this procedure is 1,000 heavy-tailed distributions, each with $N = 1000$. Figure S8 displays the results. As postulated, the CPC remains sensitive to component standard deviations (seen in plot (b)), but the rapid increase in WSS as a result of the heavy-tailed data overwhelms an increase in BSS and makes the measure insensitive to component means (seen in plot (a)). The performance of the other measures is similarly mixed. Difference and variance perform closer to expectations on the intergroup heterogeneity feature (plot a), but both extant measures move in the wrong direction in response to varying standard deviations (plot b).

These problems can be partially ameliorated, however, by taking the natural log of the data (between steps 3 and 4 of the simulation procedures). While this transformation maintains the heavy-tailed nature of the simulated distribution, it maps it to an interval that decreases the absolute value of the outlier observations and makes it more manageable for the sums of squares used to calculate the CPC. Figure S9

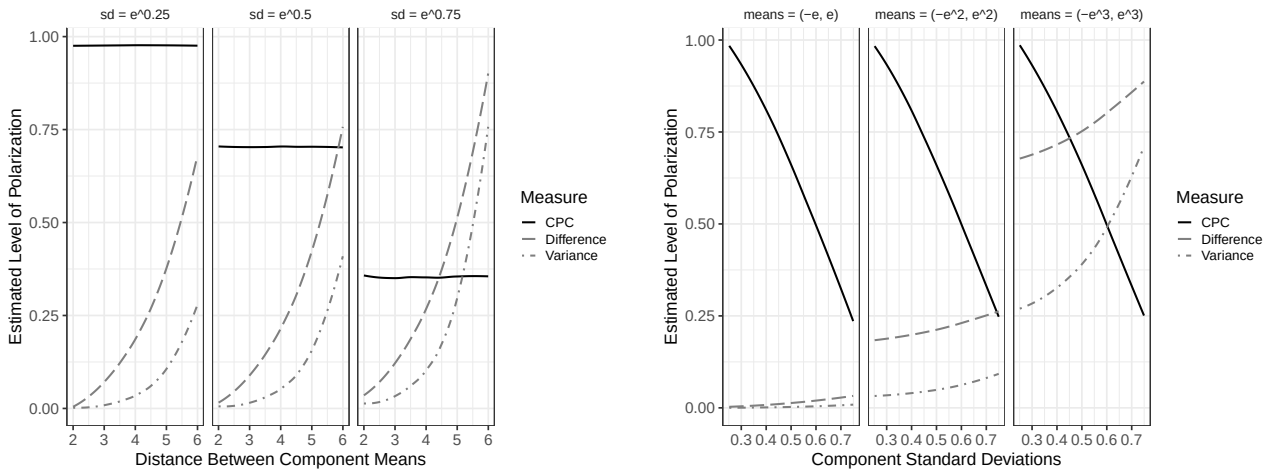

(a) Varying μ (intergroup heterogeneity)

(b) Varying σ (intragroup homogeneity)

Figure S8: Polarization Estimates with Log-Normal Data. Results from univariate simulations of polarization measures with two components, showing estimated level of polarization for a randomly varying distribution parameter, holding the other parameter constant. All measures scaled to $[0, 1]$ to enable comparison and plotted using LOESS.

displays the results of applying each measure to the transformed data. The CPC displays behavior much more in line with expectations on both features, and the other measures generally improve as well, although they all still struggle to capture the intragroup homogeneity feature (plot (b)). This underscores the need for analysts to be aware of the distribution of their data. Although distributions of real-world data may not often display heavy-tailed behavior to the extent that this simulated data does, the measure can still be vulnerable to extreme outliers. Researchers should apply appropriate transformations to their data before estimating polarization, just as they would before fitting a linear model or conducting other types of analyses.

S3.5 Results with Unequal Component Weights

I noted in section S4.1 that I maintain equal component weights in the simulations to aid in identification. This could raise concerns that results are at least partially dependent on an assumption that may not be reasonable in many real-world applications. To evaluate the effects of this constraint, I use a similar simulation framework as in section S4.1, but hold μ and σ constant and instead randomize cluster weights. Simulations to evaluate polarization measures on the intergroup heterogeneity feature follow the procedure below:

1. Fix component means at $(-3, 3)$, a middling level of polarization in this simulation framework.
2. Fix component standard deviations at a range of values $\sigma \in \{0.5, 1, 1.5, 2\}$. For identification, I use the same σ for each component and maintain a global mean of zero.
3. For each component, draw a set of component weights ϕ_K as independent draws from $\mathrm{U}(0, 1)$, such that $\sum_{k=1}^{2} \phi_k = 1$.
4. Take 1,000 independent draws from a Gaussian mixture parameterized by $\mathrm{N}(\phi_1, -\mu, \sigma; \phi_2, \mu, \sigma)$.
5. Apply each polarization measure to the resulting distribution.

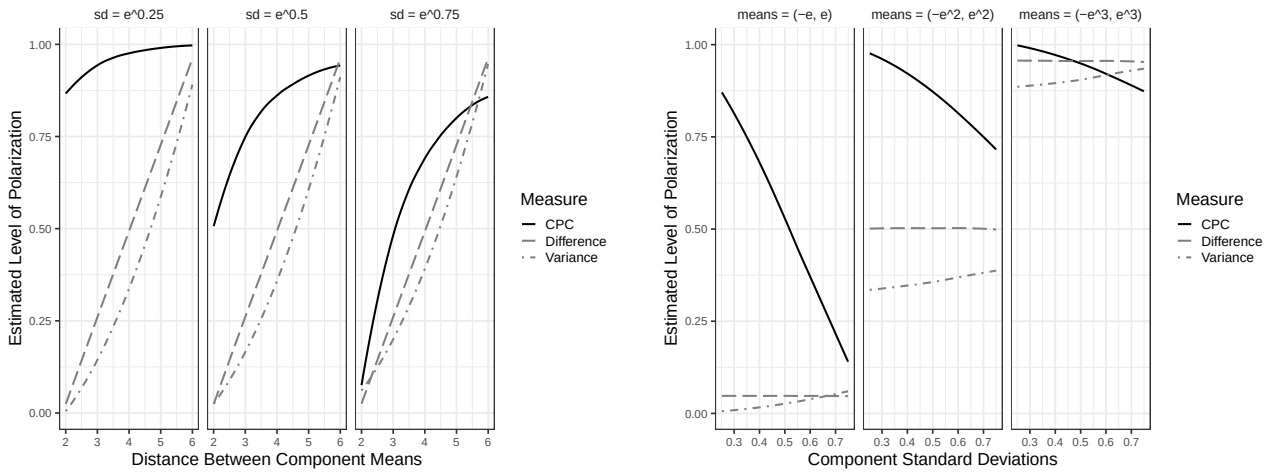

(a) Varying μ (intergroup heterogeneity)

(b) Varying σ (intragroup homogeneity)

Figure S9: Polarization Estimates with Transformed Log-Normal Data. Results from univariate simulations of polarization measures with two components, showing estimated level of polarization for a randomly varying distribution parameter, holding the other parameter constant and transforming the log-normal data using the natural log. All measures scaled to $[0, 1]$ to enable comparison and plotted using LOESS.

The result of this procedure is 1,000 distributions, each with $N = 1000$. Simulations to evaluate polarization measures on the intragroup homogeneity feature follow the procedure below:

1. Fix component standard deviations at 1, a middling level of polarization in this simulation framework.
2. Fix component means at a range of values $\mu \in \{2, 3, 4, 5\}$. For identification, I use the same absolute value of μ for each component and maintain a global mean of zero.
3. For each component, draw a set of component weights ϕ_K as independent draws from $\mathrm{U}(0, 1)$, such that $\sum_{k=1}^{2} \phi_k = 1$.
4. Take 1,000 independent draws from a Gaussian mixture parameterized by $\mathrm{N}(\phi_1, -\mu, \sigma; \phi_2, \mu, \sigma)$.
5. Apply each polarization measure to the resulting distribution.

The result of this procedure is 1,000 distributions, each with $N = 1000$.

For each set of simulations, I then plot estimated polarization as a function of the difference between the two component weights. As in all other simulations, I calculate the CPC using the true cluster memberships, which are known from the data randomization procedure. Figure S10 displays the results. As expected, the adjusted CPC is relatively invariant to the difference in component weights except when that difference is high, at which point the mixture distribution approaches unimodality and the CPC decreases precipitously.

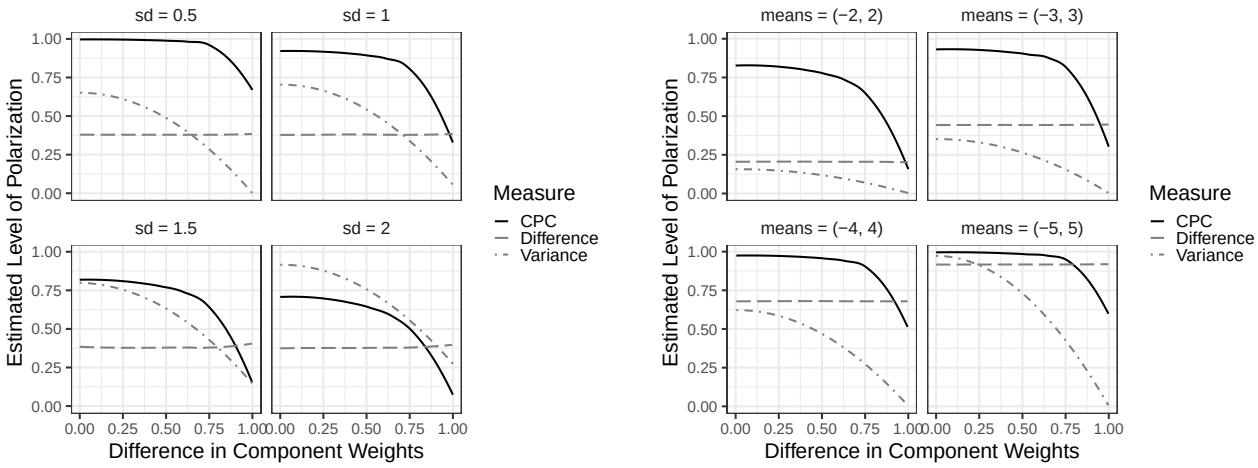

(a) Varying μ (intergroup heterogeneity)

(b) Varying σ (intragroup homogeneity)

Figure S10: Univariate Polarization Estimates with Two Components. Results from univariate simulations of polarization measures with two components, showing estimated level of polarization for randomly varying component weights, holding distribution parameters constant. All measures scaled to $[0, 1]$ to enable comparison and plotted using LOESS.

S4 Benchmarking Against Human Coders

The simulation evidence presented in the previous section is helpful for ensuring the CPC responds in theoretically appropriate ways to changes in distributional features. However, the lack of ground-truth polarization labels makes it difficult to judge whether the CPC is a more accurate measure of polarization compared to others. Recovering a ranking of distributions based on randomized distribution parameters comes close to solving that problem, but in these simulations, only one feature can be manipulated at a time. In real-world data, both features vary simultaneously, often independent of each other. I therefore use human coders to gather ground-truth annotations of distributions' level of polarization, against which I can benchmark each measure's performance.

I first generated fifty bimodal distributions using the same parameters as in section S4.1, randomly varying both component means and standard deviations at the same time. To make the task more accessible to non-experts, I colored one component blue and one component red and referred to them as graphs of Democratic and Republican ideology. The full task preamble and sample graphs can be seen in Figure S11.

After the preamble, coders answered three screening questions to ensure they understood the task. These screening questions were identical to those they saw in the main task, but I chose the graphs presented in the screening questions such that one was obviously more polarized than the other. Coders were only allowed to complete the main task if they answered all three screening questions correctly. I explicitly told coders that polarization involved both features and tested them on that knowledge with easy screening questions for two reasons. First, I wanted to make sure coders understood the task. Second, I was not concerned with how the coders themselves thought about polarization, only that they could evaluate polarization according to the two-feature definition while *both* features varied across distributions—something I could not achieve in the simulations. For those coders who passed the screening questions, I randomly selected twenty pairs of plots, presented them to the coders, and asked them: "Which of the two graphs below is more polarized?"

Lots of people have noticed that American politics have become more polarized in recent years. Polarization means that Democrats have ideologies that are very similar to other Democrats' ideologies and very different from Republicans' ideologies, and vice versa.

We need to collect data about what this polarization looks like in graphs of Democrats' and Republicans' ideologies. We will show you 20 pairs of graphs like the ones below. In this pair, the graph on the right (or on the bottom if viewing on a mobile device) is more polarized because Democrats' (blue) and Republicans' (red) ideologies are farther apart and each party's members have ideologies that are more similar to others in their party. Your task will be to tell us which of the two graphs looks more polarized in each of the 20 pairs.

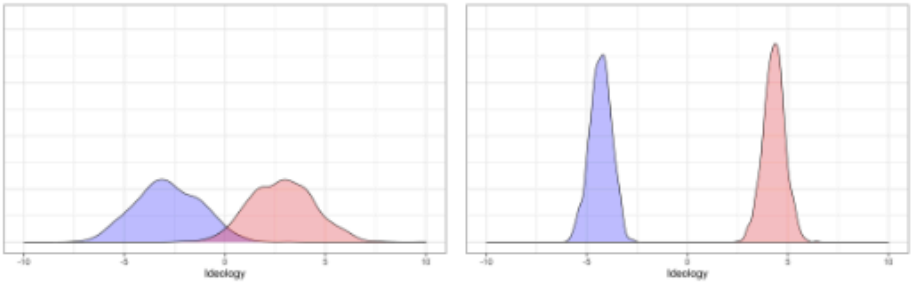

Figure S11: Preamble and Sample Graphs of Polarization Labeling Task

The result of each coder's task was therefore twenty random pairwise comparisons labeled according to which of the two options was more polarized. 495 workers on Amazon's Mechanical Turk completed the task.[16] From the pairwise comparisons, a log-linear Bradley-Terry model recovered a ranking of distributions according to their level of polarization (Bradley and Terry 1952). I then applied each measure of polarization to all distributions and again ranked them according to the level of estimated polarization. The outcome of this exercise, then, is four rankings of fifty distributions: one set of rankings uncovered by measures of difference, variance, and the CPC, and one set of rankings recovered from human coding to be treated as ground-truth information.

	Difference	Variance	CPC
RMSE	18.17	20.381	**4.441**
Spearman's ρ	0.207	0.003	**0.953**

Table S4: Benchmark of Polarization Measurements Against Rankings Recovered from Human Coders. Root mean squared error and Spearman's ρ; bolded values denote measure with lowest error.

Table S4 describes the extent to which each polarization measure departs from the human-coded ground-truth ranking. On both root mean squared error (RMSE) and Spearman's ρ, the CPC gives a more accurate approximation of the human-coded ranking, with RMSE less than one third the size of difference, the next most accurate measure. The CPC also achieves a very high Spearman's ρ of 0.953, while difference achieves a much lower 0.207 and variance registers almost no correlation at all with the human-coded ground-truth

16. In addition to passing the three screening questions, workers were required to be over age 18, located in the United States, and have at least a 95% approval record on more than fifty completed MTurk tasks.

ranking. These results suggest that the CPC's ability to capture the two theoretical features of polarization extends to cases where both features vary simultaneously.

S4.1 Data Collection and Ethics

The human-coded data used in this section was collected in accordance with the American Political Science Association's standards for professional ethics and principles for human subjects research. Data collection and handling protocols were approved by an Institutional Review Board. The data collection task was programmed in Qualtrics and distributed to workers recruited through Amazon's Mechanical Turk crowdsourcing platform. Respondents are all Americans aged 18 years or older. Vulnerable populations (e.g. prisoners, respondents with a direct-dependency relationship with the researchers, decisionally impaired individuals, etc.) were unlikely to be included as respondents.

Prior to beginning the study, all respondents were informed of potential risks (consequences of breach of confidentiality) in a process of informed consent. They were also informed that they had the right to refuse the study, opt out of the study at any time, or withdraw their data after completing the survey. The task was approximately two minutes in length. Workers were paid $0.35 for the task, making worker compensation similar to what they could expect to earn for an equivalent amount of work at a minimum-wage job in most US cities.

The data set contains no personal identifiers. A randomly generated identifier with no relation to actual identifiers was generated by the Qualtrics software and used to connect each completed survey response to the Worker ID (a random alphanumeric string assigned by Amazon) of the individual who completed it. No demographic data was collected, so deductive disclosure was not possible.

S5 Cross-National Polarization Application

S5.1 Selecting Number of Clusters

As noted in the main text, one challenge in using clustering methods is the need to specify the number of clusters n_k. Although Figure 3A in the main text makes this selection relatively clear, I use silhouette scores to confirm the appropriate number of clusters in each distribution. This method involves repeatedly running the clustering algorithm with an increasingly large number of clusters. For each n_k, a "silhouette score" is then calculated. Silhouette scores use an arbitrary distance metric to determine how similar each point is to its own cluster and how different it is from other clusters. These individual scores are then aggregated into a value in the range $[-1, 1]$, where -1 implies the worst possible fit and 1 implies the best possible fit. The number of clusters which produces the maximum silhouette score is the most appropriate value for n_k. Figure S12 displays silhouette plots for each country. There is a clear maximum value for each country, corresponding to a two-cluster specification in Germany, Italy, the United States, and the United Kingdom, and three-cluster specifications in the Netherlands and Spain.

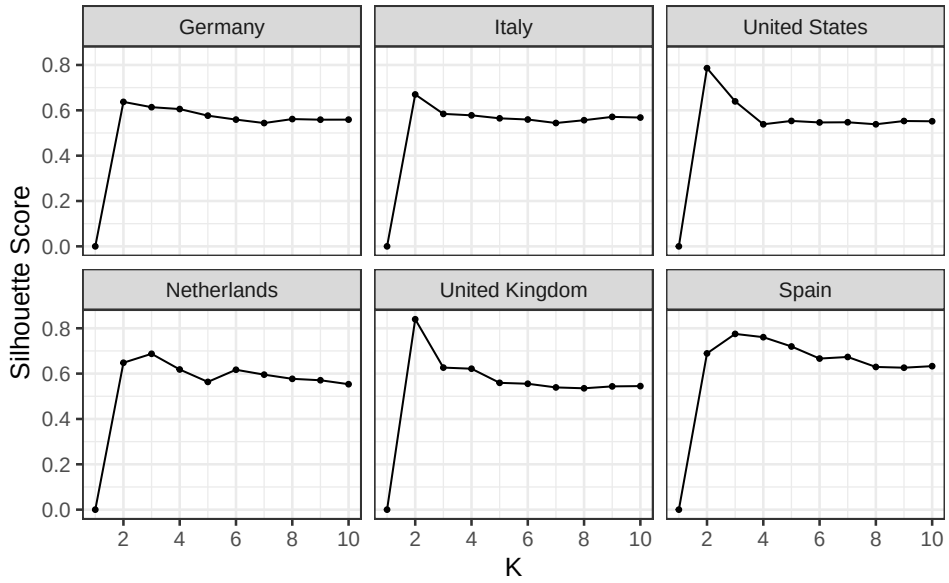

Figure S12: Silhouette Scores of Ideology Estimates by Country

S5.2 Robustness to Clustering Method

The CPC and difference-in-means measures require knowledge of the group to which each observation belongs, so I use three different unsupervised clustering methods to assign observations to clusters within each country. The first method is k-means clustering, which iteratively assigns observations to the nearest cluster centroid (Hartigan and Wong 1979). The results reported in the main text use cluster memberships recovered from this method.

To ensure polarization results are not merely artifacts of this particular approach to recovering cluster memberships, I also implement both agglomerative and divisive hierarchical clustering algorithms. Agglomerative clustering with complete linkage begins by assigning each observation to its own cluster. At each iteration, the algorithm then merges the two clusters with the shortest distance between each other. The distance $D(A, B)$ between clusters A and B is determined by $D(A, B) = \max_{x \in X, y \in Y} d(x, y)$, where $d(x, y)$ is the distance between x and y (Defays 1977).

Divisive clustering, on the other hand, begins by assigning all observations to the same group. At each iteration, the algorithm selects the cluster with the largest distance between its members and finds the observation in that cluster with the largest average distance to all other observations in that cluster. This observation becomes the first observation in the "splinter group." The algorithm then divides the selected cluster into two clusters by assigning observations either to the existing cluster or the splinter group based, again, on average distance to all observations in each cluster (Kaufman and Rousseeuw 2005).

Figure S13 displays polarization estimates generated by the CPC (top row) and difference-in-means (bottom row) with cluster memberships recovered from k-means, complete-linkage agglomerative clustering, and divisive clustering. Countries are ordered by CPC estimates and error bars give 95% confidence intervals. Other than wider confidence intervals in the case of agglomerative clustering, results are consistent across all three clustering methods. In each case, the CPC recovers the same ordering presented in the main text, showing Germany and Italy with the lowest levels of polarization, the United States, Netherlands, and United

Kingdom with higher levels, and Spain with the highest level overall. Difference-in-means estimates are also consistent, with the United Kingdom appearing by far the most polarized, followed by Italy, the Netherlands, Spain, Germany, and the United States as the least polarized. These consistent results reassure me that the polarization levels reported in the main text are not merely a mechanical result due to the specific clustering algorithm used.

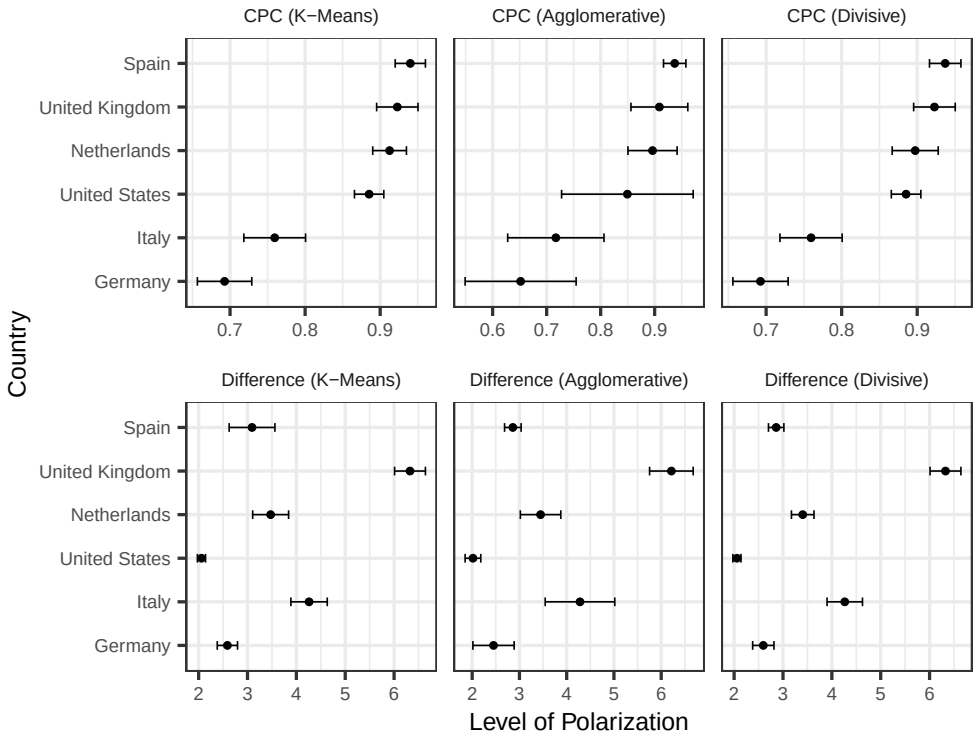

Figure S13: CPC and Difference-in-Means Estimates Across Clustering Methods. Error bars give 95% confidence intervals, calculated using a case-resampling bootstrap.

S5.3 Full Polarization Estimates

Table S5 displays the polarization estimates and associated standard errors for each country and measure presented in the analysis of elite ideological ideal points in the main text. The estimates in Table S5 correspond to Figure 3B in the main text.

	Measure			
	Difference	Variance	CPC	Expert-Coded
Germany	2.59	1.9	0.696	0.337
	(0.115)	(0.112)	(0.023)	
Italy	4.25	5.07	0.758	0.319
	(0.187)	(0.404)	(0.022)	
Netherlands	3.45	3.98	0.91	0.382
	(0.175)	(0.36)	(0.013)	
Spain	3.09	2.28	0.94	0.474
	(0.231)	(0.232)	(0.01)	
United Kingdom	6.38	9.82	0.924	0.38
	(0.17)	(0.646)	(0.015)	
United States	2.06	1.17	0.885	0.376
	(0.043)	(0.047)	(0.009)	

Table S5: Polarization Estimates and Associated Standard Errors from Analysis of Cross-National Elite Ideal Points. Corresponds to main text Figure 3B. Standard errors are in parentheses

S6 Affective Polarization Application

S6.1 Polarization Estimates

Figure S14 displays estimated levels of affective polarization across all twenty-eight countries in the sample, according to each measure. Countries are ordered by their estimated level of polarization as measured by the CPC.

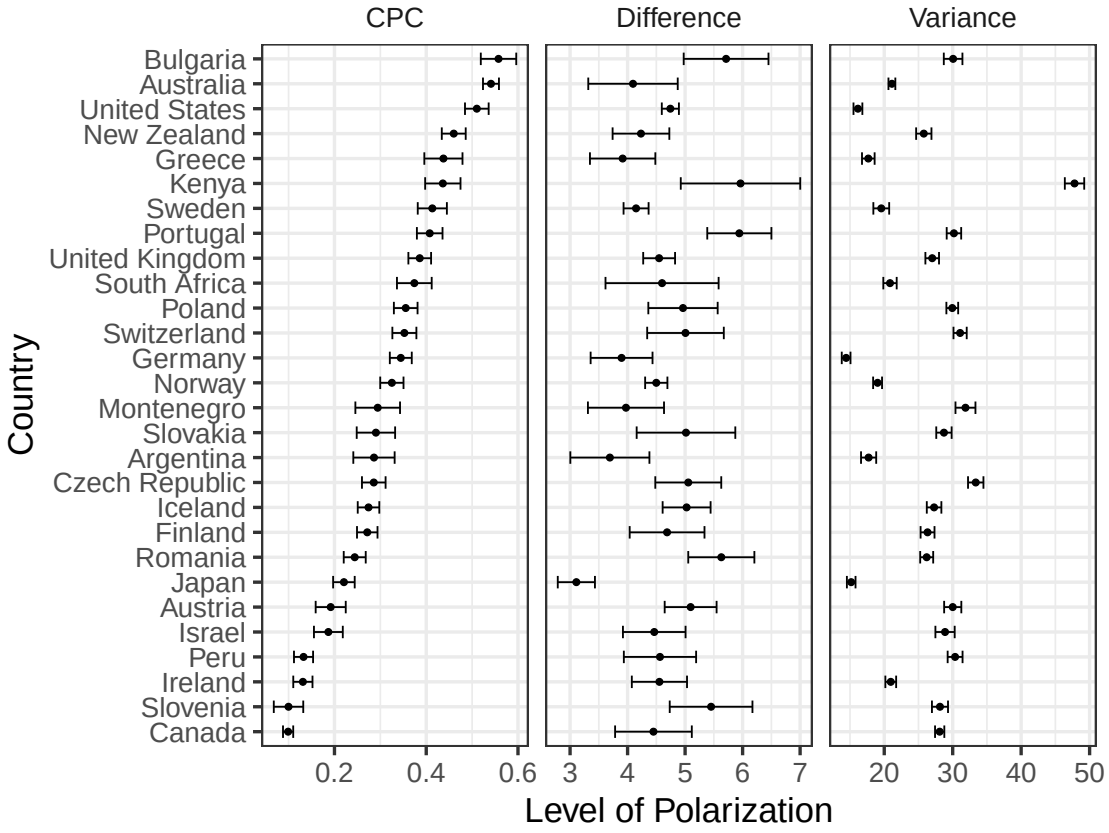

Figure S14: Affective Polarization Levels Across Countries. Error bars give 95% confidence intervals, calculated using a case-resampling bootstrap.

S6.2 Full Correlation Results

Table S6 displays estimated correlations between affective polarization estimates and the additional variables discussed in the main text, along with the standard errors of those correlations. The estimates in Table S6 correspond to Figure 4 in the main text.

	Measure		
	Difference	Variance	CPC
Who in Power Makes Difference	0.116	-0.078	0.313
	(0.051)	(0.025)	(0.012)
Vote Makes Difference	-0.044	-0.256	0.319
	(0.046)	(0.033)	(0.017)
Very Close to Party	-0.283	-0.521	0.336
	(0.039)	(0.031)	(0.033)
Ideological Extremity	0.399	0.467	0.252
	(0.036)	(0.035)	(0.037)

Table S6: Correlates of Affective Polarization. Corresponds to main text Figure 4. Standard errors are in parentheses

S6.3 Weight of Features on CPC Estimates

Some of the simulation results in section S3 suggest that the CPC may be more heavily influenced by one feature than the other, depending on the relative levels of each. To evaluate the relative weight of each feature on CPC estimates, I randomly vary each feature across a range of values that might be seen in real-world data, using the party affect data from above to define this plausible range of values.

To do so, I take data from three countries—Canada (lowest estimated polarization), Bulgaria (highest estimated polarization), and Norway (approximate midpoint between Canada's and Bulgaria's polarization levels)—and calculate BSS and WSS separately for each. Using each estimate of BSS and WSS (low, medium, and high), I then take 1,000 independent draws from $\text{U}(\frac{BSS}{2}, \frac{3BSS}{2})$ and $\text{U}(\frac{WSS}{2}, \frac{3WSS}{2})$. This exercise therefore allows me to randomly vary each feature *simultaneously* over a range of plausible values (something I could not do in the simulations above), while still ensuring that each feature varies independent of the other—an important attribute for determining the relative weight of each feature on the CPC, which is calculated from these two values.

I begin with descriptive evidence in Figure S15, which plots the value of each feature against the CPC value they combine to produce. As expected, the CPC increases as BSS increases and decreases as WSS increases. The relationship between each feature and the CPC appears more linear than in some of the simulations above, but there does appear to be some evidence of diminishing returns to BSS at high levels of polarization and to WSS at low levels of polarization, consistent with simulation results.

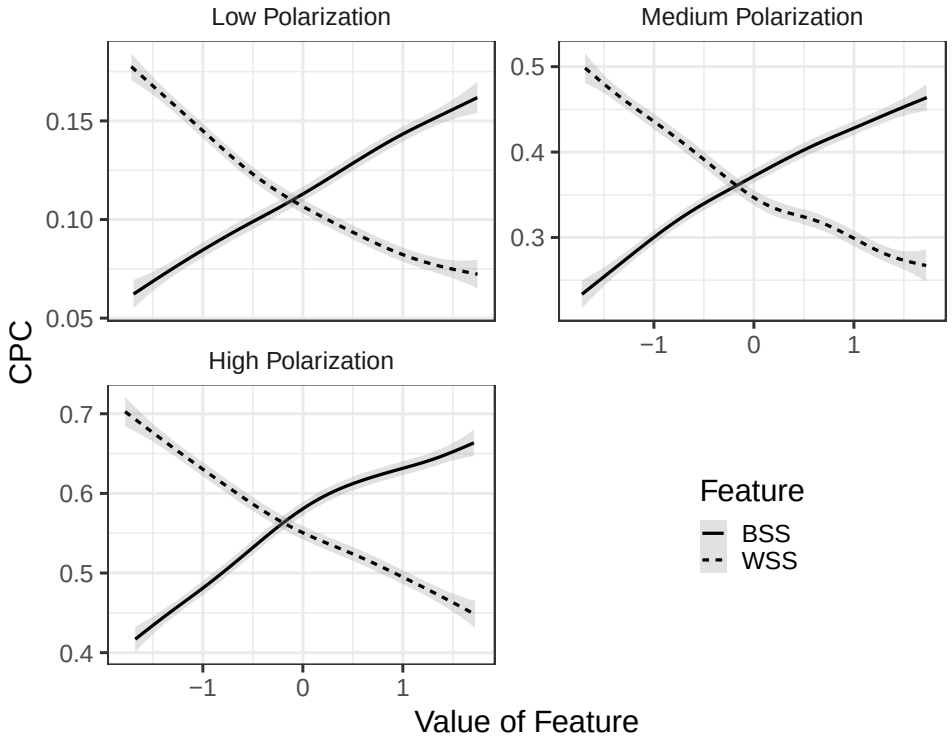

Figure S15: Changes in CPC Estimates with Independent Changes in Individual Features. Values of features unit-normalized to enable comparison.

More important, though, is to understand the *ceteris paribus* effect of each feature on the CPC. To investigate this, I fit OLS models of CPC estimates on BSS and WSS. Table S7 presents the results of these models. The coefficient magnitudes on BSS and WSS are very similar in all three models, giving some reassurance that the CPC is not being overwhelmingly driven by one feature more than the other. However, the faint diminishing returns observed in Figure S15 also show up in these results. The absolute magnitude of the WSS coefficient is greater than that of the BSS coeffiicient in cases of low and mid-range polarization. But when the overall level of polarization is high, that relationship flips, and the absolute magnitude of the BSS coefficient is greater than that of the WSS coefficient.

	Dependent variable:		
	CPC		
	Low Polarization	Medium Polarization	High Polarization
	(1)	(2)	(3)
BSS	0.029*	0.067*	0.075*
	(0.0003)	(0.0005)	(0.0005)
WSS	−0.031*	−0.070*	−0.071*
	(0.0003)	(0.0005)	(0.0005)
Constant	0.113*	0.364*	0.561*
	(0.0003)	(0.0005)	(0.0005)
Observations	1,000	1,000	1,000
R^2	0.945	0.978	0.981
Adjusted R^2	0.945	0.978	0.981
Residual Std. Error (df = 997)	0.010	0.014	0.014
F Statistic (df = 2; 997)	8,539.664*	21,929.600*	25,297.340*
Note:			*p<0.05

Table S7: Effect of Individual Features on CPC Estimates. BSS and WSS unit-normalized. Standard errors in parentheses.

These diminishing returns and their dependence on overall polarization can be seen more clearly in the added-variable plots in Figure S16. These plots use the models from Table S7 to assess the impact of each feature on the CPC while holding the other feature constant. Plots are separated into pairs according to low-, medium-, and high-polarization contexts. Within each pair of plots, the facet on the left displays the effect of BSS on the CPC, given WSS. The facet on the right displays the effect of WSS on the CPC, given BSS. Figure S16, plot (b) shows an approximately linear effect for both BSS and WSS on the CPC at a medium level of polarization. Just to the left, in Figure S16, plot (a), this linear effect appears again in the case of BSS, but WSS displays a diminishing effect, suggesting that BSS carries greater weight in the calculation of the CPC when the overall level of polarization is low. The opposite is true in Figure S16, plot (c), which reveals a linear effect of WSS on the CPC, but a diminishing effect of BSS, suggesting that the former carries greater weight when the overall level of polarization is high. However, in neither case does this diminishing effect appear to be substantial.

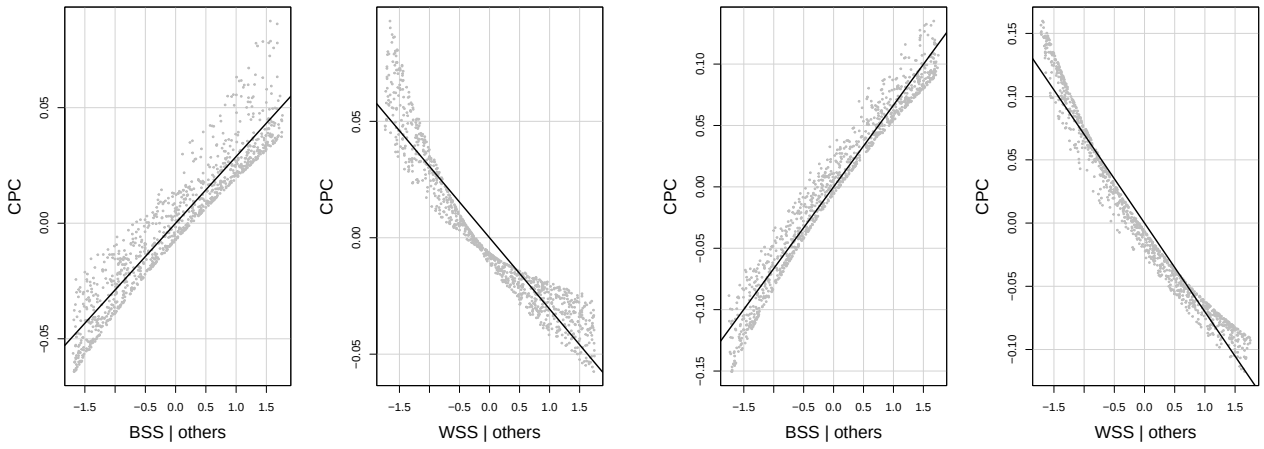

(a) Low Polarization

(b) Medium Polarization

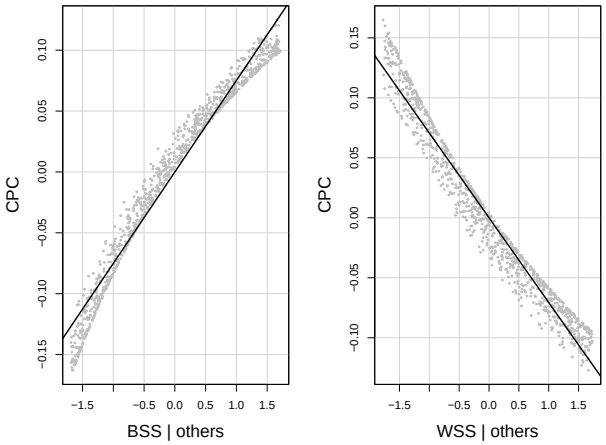

(c) High Polarization

Figure S16: Added-Variable Plots of Polarization Features and CPC Estimates. Values of features unit-normalized to enable comparison.

Taking into account all results presented in this section and in the simulations, the preponderance of evidence points toward three conclusions: First, the contributions of each feature to CPC estimates are comparable, at least over a range of values observed in real-world data. Second, BSS may contribute more heavily in cases of low polarization, but this difference is not substantial. Third, WSS may contribute more heavily in cases of high polarization, but this difference is, again, not substantial.

References

Bradley, Ralph Allan, and Milton E. Terry. 1952. "Rank Analysis of Incomplete Block Designs: I. The Method of Paired Comparisons." *Biometrika* 39, nos. 3/4 (December): 324.

Defays, D. 1977. "An Efficient Algorithm for a Complete Link Method." *The Computer Journal* 20, no. 4 (January): 364–366.

Hartigan, J. A., and M. A. Wong. 1979. "Algorithm AS 136: A K-Means Clustering Algorithm." *Journal of the Royal Statistical Society, Series C (Applied Statistics)* 28 (1): 100–108.

Kaufman, Leonard, and Peter J. Rousseeuw. 2005. *Finding Groups in Data: An Introduction to Cluster Analysis.* Wiley Series in Probability and Mathematical Statistics. Hoboken, NJ: Wiley.

Lupu, Noam, Lucía Selios, and Zach Warner. 2017. "A New Measure of Congruence: The Earth Mover's Distance." *Political Analysis* 25, no. 1 (January): 95–113.

Magee, Lonnie. 1990. "R2 Measures Based on Wald and Likelihood Ratio Joint Significance Tests." *The American Statistician* 44, no. 3 (August): 250–253.